Evaluation of S^2 for correlated wave functions and spin projection of unrestricted Møller–Plesset perturbation theory

Wei Chen[a] and H. Bernhard Schlegel[b]
Department of Chemistry, Wayne State University, Detroit, Michigan 48202

(Received 10 March 1994; accepted 9 May 1994)

The value of S^2 can be an important diagnostic tool for judging the quality of correlated wave functions. A production code has been developed to evaluate S^2 for unrestricted Møller–Plesset perturbation theory (UMPn), coupled clusters (UCCSD), quadratic configuration interaction (UQCISD), and Brueckner doubles (UBD) methods, and to evaluate UMP3 and UMP4 energies with spin projection. The code has been used to examine the bond dissociation potentials for $HF \rightarrow H+F$ and $CH_4 \rightarrow CH_3+H$. For both systems, the onset of the RBD-UBD instabitity occurs near $S^2 \approx 0.35$ for UCCSD or UQCISD calculations. Maximum errors in the UMP4, UCCSD(T), UQCISD(T), and UBD(T) single bond dissociation curves are near $S^2 \approx 0.5$. The behavior of S^2 for UCCSD and UQCISD is closer to BD than MP4. Projected MP4 energies are in good agreement with full CI calculations, but between the onset of the RHF-UHF instability and the RBD-UBD instability, CCSD(T), QCISD(T), and BD(T) are significantly better. If $A_{\text{Norm}} > 1.2$ for restricted calculations on single bond dissociations, it is better to use a spin-unrestricted method.

INTRODUCTION

Spin-unrestricted Hartree–Fock[1] (UHF) and post-SCF methods based on UHF references such as unrestricted Møller–Plesset perturbation theory[2] (UMPn), unrestricted coupled clusters theory[3] (UCC), and unrestricted quadratic configuration interaction theory[4] (UQCI) have been widely used for open shell systems. In recent years, unrestricted Brueckner doubles[5] (UBD) has also become available for open shell systems. Spin-unrestricted methods are usually quite reliable and yield satisfactory energies and optimized geometries. In addition, they approach the correct limit for the bond dissociation in the closed shell systems,[6] while spin-restricted Hartree–Fock[7] (RHF) and spin-restricted post-SCF methods can give the incorrect results when bonds are stretched far away from the equilibrium geometries. Unrestricted methods also give reasonable spin densities for open shell systems, whereas restricted methods require more extensive configuration interaction for an acceptable description of spin densities.[8,9]

The major shortcoming of the UHF and unrestricted post-SCF methods is that the wave functions are not eigenfunctions of the spin operator S^2. Frequently this is not a problem, since the contributions from higher spin states are often small. However, there are circumstances where the spin contamination can be large enough to adversely effect the shape of the calculated energy surface and the magnitude of the spin densities. The amount of spin contamination can be determined from $\langle S^2 \rangle$. Most electronic structure programs (e.g. Ref. 10) evaluate $\langle S^2 \rangle$ for simple methods such as UHF and UMP2, but there is a need to calculate $\langle S^2 \rangle$ for higher order Møller–Plesset perturbation theory and for more accurate methods of treating electron correlation. The first part of this paper deals with the calculation of S^2 for unrestricted, single reference post-SCF theories, and its use as a diagnostic tool in assessing the quality of these calculations.

The second part of this paper is concerned with the treatment of the spin contamination problem. A number of approaches have been used, including restricted open shell Hartree–Fock (ROHF) and spin-restricted multiconfiguration self-consistent field[11] (MCSCF) as well as spin projection methods. Since ROHF theory uses the same set of spatial orbitals for the alpha and beta spin orbitals, the wave function is an eigenfunction of S^2. Hence ROHF has no spin contamination for the open shell systems. Restricted open shell Møller–Plesset perturbation theory and coupled-cluster methods for electron correlation have been implemented recently by Pople, Handy,[12,13] and Bartlett.[14] Although single reference spin-restricted methods are very useful for open shell calculations, they are not suitable for the calculation of bond dissociation potential energy curves. The MCSCF approach is perhaps the best choice since multiple reference determinants are used, but it is limited to smaller systems than single reference post-SCF calculations and corrections for dynamic correlation are more difficult. An alternative method is spin projection of unrestricted Hartree–Fock and post-SCF theories. Spin projection of UHF calculations was discussed a number of decades ago by Löwdin[15] and Amos and Hall.[16] Several years ago we demonstrated that an approximate spin projected UMPn method was very effective in treating the problem of extremely slow convergence of unrestricted Møller–Plesset perturbation theory for cases with serious spin contamination in the UHF reference determinant.[17] Two similar methods for calculating fully spin projected unrestricted Møller–Plesset perturbation (proj UMPn) energies were proposed by Handy[18] and ourselves;[19] these methods were tested by comparison with full configuration interaction (FCI) calculations. Because matrix elements such as $\langle \Psi_u | S^2 | \Psi_v \rangle$ are difficult to evaluate for u and v equal to double, triple, and quadruple excitations, these two methods have been implemented only at the UMP2 level of the theory for practical applications. In this paper we discuss

[a]Current address: Department of Chemistry, Iowa State University, Ames, Iowa 50011.
[b]Author to whom correspondence should be addressed.

the implementation of spin projected UMP3 and UMP4 methods, and compare spin projected UMPn results with other higher levels of calculations such as UCC, UQCI, and UBD on the single bond dissociation curves of HF and CH_4 systems.

S^2 for post-SCF methods

The expectation value of S^2 is

$$\langle S^2\rangle=\langle\Psi|S^2|\Psi\rangle/\langle\Psi|\Psi\rangle. \tag{1}$$

For most post-SCF methods, the wave function can be partitioned into a reference determinant, Ψ_0, and a correlation correction, $\Psi_{\rm corr}$, that can be expanded as a sum over single, double, triple, quadruple, and higher multiple excitations:

$$\Psi=\Psi_0+\Psi_{\rm corr},\quad \Psi_{\rm corr}=\sum_S a_S\Psi_S+\sum_D a_D\Psi_D+\sum_T a_T\Psi_T+\sum_Q a_Q\Psi_Q+\cdots. \tag{2}$$

For many post-SCF methods, evaluation of Eq. (1) requires the matrix elements $\langle\Psi_u|S^2|\Psi_v\rangle$, where u and v are triple or higher excitations. This is rather complicated and CPU time consuming; hence, Eq. (1) is generally not used in practical calculations.

Alternatively, one can add a perturbation λS^2 to the Hamiltonian and evaluate S^2 as

$$\langle S^2\rangle=\left.\frac{dE(\lambda)}{d\lambda}\right|_{\lambda=0}. \tag{3}$$

Note that Eq. (3) is generally not equivalent to Eq. (1) if the wave function does not satisfy the Hellmann–Feynman theorem, i.e., Eqs. (1) and (3) are equivalent for Hartree–Fock and CASSCF methods, but not for a number of post-SCF methods such as MPn, CC, QCI, etc.

The value of S^2 for UMPn defined by Eq. (3) can be written as

$$\langle S^2\rangle=\sum_{i=0}^{n-1}\langle S^2\rangle_i,\quad \langle S^2\rangle_i=\left.\frac{dE_{i+1}(\lambda)}{d\lambda}\right|_{\lambda=0}, \tag{4}$$

where $\langle S^2\rangle_i$ is the value for the ith order wave function which corresponds to the $(i+1)$th order perturbation energy E_{i+1}. Up to third order (i.e., MP4 energy), this yields

$$\begin{aligned}\langle S^2\rangle_1&=2\langle\Psi_0|S^2|\Psi_1\rangle\\ \langle S^2\rangle_2&=2\langle\Psi_0|S^2|\Psi_2\rangle+\langle\Psi_1|S^2|\Psi_1\rangle-\langle\Psi_1|\Psi_1\rangle\langle S^2\rangle_0,\\ \langle S^2\rangle_3&=2\langle\Psi_0|S^2|\Psi_3\rangle+2\langle\Psi_1|S^2|\Psi_2\rangle-\langle\Psi_1|\Psi_1\rangle\langle S^2\rangle_1\\ &\quad-2\langle\Psi_1|\Psi_2\rangle\langle S^2\rangle_0,\end{aligned} \tag{5}$$

where $\langle S^2\rangle_0=\langle\Psi_0|S^2|\Psi_0\rangle$, the UHF expectation value of S^2. Equation (5) can also be obtained from Eq. (1) by expanding the denominator and collecting the ith order terms. Since S^2 is a two electron operator and Ψ_1 involves only double excitation, Eq. (5) contains only two types of matrix element calculations: $\langle\Psi_0|S^2|\Psi_u\rangle$ $(u=S,\ D)$ and $\langle\Psi_u|S^2|\Psi_v\rangle$ $(u=D,\ v=S,\ D,\ T,$ and $Q)$. The nonzero elements of these matrices are listed in Table I. The computational effort required to evaluate S^2 is similar to that required for the energy [i.e., $O(N^6)$ for MP3, $O(N^7)$ for MP4].

The total energies and wave functions for truncated configuration interaction (CID, CISD), coupled clusters (CCD, CCSD), quadratic configuration interaction (QCISD), and Brueckner doubles (BD) methods can generally be expressed as

$$E=\langle\Psi_0|\mathbf{H}|\Psi\rangle,\qquad \Psi=\Psi_0+\Psi_{\rm corr}=\Psi_0+\sum_u a_i^a\Psi_i^a+\sum_u a_{ij}^{ab}\Psi_{ij}^{ab}+\cdots, \tag{6}$$

$$\langle\Psi_0|\bar{\mathbf{H}}|\Psi\rangle=E_{\rm corr},\qquad \langle\Psi_i^a|\bar{\mathbf{H}}|\Psi\rangle=a_i^aE_{\rm corr},\quad \langle\Psi_{ij}^{ab}|\bar{\mathbf{H}}|\Psi\rangle=a_{ij}^{ab}E_{\rm corr}, \tag{7}$$

where Ψ_0 is the reference determinant; Ψ_i^a, Ψ_{ij}^{ab} are determinants that are singly, doubly excited, etc. The CID and CISD wave functions are $\Psi_{\rm CID}=(1+\mathbf{T}_2)\ \Psi_0$ and $\Psi_{\rm CISD}=(1+\mathbf{T}_1+\mathbf{T}_2)\ \Psi_0$, respectively. The substitution operators $\mathbf{T}_1=\Sigma\ a_i^a\mathbf{t}_i^a$ and $\mathbf{T}_2=\Sigma\ a_{ij}^{ab}\mathbf{t}_{ij}^{ab}$ can be express in terms of the elementary substitution operators (e.g., $\mathbf{t}_i^a$ replaces occupied spin orbital ϕ_i by unoccupied spin orbital ϕ_a, etc.). In the CCD and CCSD approaches, $\Psi_{\rm CCD}=\exp(\mathbf{T}_2)\ \Psi_0$ and $\Psi_{\rm CCSD}=\exp(\mathbf{T}_1+\mathbf{T}_2')\ \Psi_0$, respectively $(\mathbf{T}_2'=\mathbf{T}_2-\frac{1}{2}\mathbf{T}_1^2)$. In the quadratic configuration interaction singles and doubles method (QCISD), only the minimum number of excitation operators are added to the CI equations to make them size-consistent:

$$\langle\Psi_0|\mathbf{H}|\mathbf{T}_2\Psi_0\rangle=E_{\rm corr}, \tag{8a}$$

$$\langle\Psi_i^a|\bar{\mathbf{H}}|(\mathbf{T}_1+\mathbf{T}_2+\mathbf{T}_1\mathbf{T}_2)\Psi_0\rangle=a_i^aE_{\rm corr}, \tag{8b}$$

$$\langle\Psi_{ij}^{ab}|\bar{\mathbf{H}}|(1+\mathbf{T}_1+\mathbf{T}_2+\tfrac{1}{2}\mathbf{T}_2^2)\Psi_0\rangle=a_{ij}^{ab}E_{\rm corr}. \tag{8c}$$

Note that there is no well-defined wave function for the QCISD method [i.e., the $\mathbf{T}_1\mathbf{T}_2$ term in Eq. (8b) is not present in Eq. (8c)].

If one chooses a reference state Φ_0 for which the single substitution coefficients a_i^a in the expression of CCSD wave function become zero, the Brueckner doubles equation is obtained:

$$\begin{aligned}&\langle\Phi_0|\mathbf{H}|(1+\mathbf{T}_2|(1+T_2)\Phi_0\rangle=E\\ &\langle\Phi_i^a|\mathbf{H}|(1+\mathbf{T}_2)\Phi_0\rangle=0,\\ &\langle\Phi_{ij}^{ab}|\mathbf{H}|(1+\mathbf{T}_2+\tfrac{1}{2}\mathbf{T}_2^2)\Phi_0\rangle=a_{ij}^{ab}E\end{aligned} \tag{9}$$

where E is the total energy. To obtain the Brueckner reference state Φ_0, a set of orbital rotations is performed so that the singles amplitudes are zero. As emphasized in the original paper,[5] the occupied-virtual block of the Fock matrix $f_{ia}=\langle\Phi_0|\mathbf{H}|\Phi_i^a\rangle$ is nonzero, and occupied–occupied and virtual–virtual blocks are not required to be diagonal.

Based on Eq. (3), S^2 for spin-unrestricted CI, CC, QCI, and BD is given by

TABLE I. Nonzero matrix elements of $\langle\Psi_0|S^2|\Psi_u\rangle$ and $\langle\Psi_{ij}^{ab}|S^2|\Psi_v\rangle$.[a]

$0\rightarrow 0$

$$\langle\Psi_0|S^2|\Psi_0\rangle=[s(s+1)+n_\beta]-\sum_{i,\tilde{j}}^{\text{occ}} S_{i\tilde{j}}S_{\tilde{j}i}$$

$0\rightarrow\alpha$ $(i,a:\alpha)$

$$\langle\Psi_0|S^2|\Psi_i^a\rangle=-T^\alpha(i,a)$$

$0\rightarrow\alpha\beta$ $(i,a:\alpha;j,b:\beta)$

$$\langle\Psi_0|S^2|\Psi_{ij}^{ab}\rangle=-U^{\alpha\beta}(i,b)U^{\beta\alpha}(j,a)$$

$\alpha\alpha\rightarrow\alpha$ $(i,j,k,a,b,c:\alpha)$

$$\langle\Psi_{ij}^{ab}|S^2|\Psi_k^c\rangle=-\delta_{ik}\delta_{ac}T^\alpha(b,j)+\delta_{jk}\delta_{ac}T^\alpha(b,i)+\delta_{ik}\delta_{bc}T^\alpha(a,j)-\delta_{jk}\delta_{bc}T^\alpha(a,i)$$

$\alpha\alpha\rightarrow\alpha\alpha$ $(i,j,k,l,a,b,c,d:\alpha)$

$$\langle\Psi_{ij}^{ab}|S^2|\Psi_{kl}^{cd}\rangle=\delta_{ik}\delta_{jl}[-\delta_{ac}T^\alpha(b,d)+\delta_{ad}T^\alpha(b,c)+\delta_{bc}T^\alpha(a,d)-\delta_{bd}T^\alpha(a,c)]+\delta_{ac}\delta_{bd}[\delta_{ik}T^\alpha(l,j)-\delta_{jk}T^\alpha(l,i)-\delta_{il}T^\alpha(k,j)+\delta_{jl}T^\alpha(k,i)]$$
$$+\delta_{ik}\delta_{jl}\delta_{ac}\delta_{bd}\langle\Psi_0|S^2|\Psi_0\rangle$$

$\alpha\alpha\rightarrow\alpha\beta$ $(i,j,k,a,b,c:\alpha;l,d:\beta)$

$$\langle\Psi_{ij}^{ab}|S^2|\Psi_{kl}^{cd}\rangle=-\delta_{ik}\delta_{ac}U^{\alpha\beta}(b,d)U^{\beta\alpha}(l,j)+\delta_{jk}\delta_{ac}U^{\alpha\beta}(b,d)U^{\beta\alpha}(l,i)+\delta_{ik}\delta_{bc}U^{\alpha\beta}(a,d)U^{\beta\alpha}(l,j)-\delta_{jk}\delta_{bc}U^{\alpha\beta}(a,d)U^{\beta\alpha}(l,i)$$

$\alpha\alpha\rightarrow\alpha\alpha\alpha$ $(i,j,k,l,m,a,b,c,d,e:\alpha)$

$$\langle\Psi_{ij}^{ab}|S^2|\Psi_{klm}^{cde}\rangle=\delta_{ac}\delta_{bd}[-\delta_{ik}\delta_{jl}T^\alpha(m,e)+\delta_{ik}\delta_{jm}T^\alpha(l,e)+\delta_{il}\delta_{jm}T^\alpha(k,e)]-\delta_{ac}\delta_{be}[-\delta_{ik}\delta_{jl}T^\alpha(m,d)+\delta_{ik}\delta_{jm}T^\alpha(l,d)+\delta_{il}\delta_{jm}T^\alpha(k,d)]$$
$$+\delta_{ad}\delta_{be}[-\delta_{ik}\delta_{jl}T^\alpha(m,c)+\delta_{ik}\delta_{jm}T^\alpha(l,c)+\delta_{il}\delta_{jm}T^\alpha(k,c)]$$

$\alpha\alpha\rightarrow\alpha\alpha\beta$ $(i,j,k,l,a,b,c,d:\alpha;m,e:\beta)$

$$\langle\Psi_{ij}^{ab}|S^2|\Psi_{klm}^{cde}\rangle=\delta_{ik}\delta_{jl}[-\delta_{ac}U^{\beta\alpha}(m,d)U^{\alpha\beta}(b,e)+\delta_{bc}U^{\beta\alpha}(m,d)U^{\alpha\beta}(a,e)+\delta_{ad}U^{\beta\alpha}(m,c)U^{\alpha\beta}(b,e)-\delta_{bd}U^{\beta\alpha}(m,c)U^{\alpha\beta}(a,e)]$$
$$-\delta_{ac}\delta_{bd}[-\delta_{ik}U^{\beta\alpha}(m,j)U^{\alpha\beta}(l,e)+\delta_{jk}U^{\beta\alpha}(m,i)U^{\alpha\beta}(l,e)+\delta_{il}U^{\beta\alpha}(m,j)U^{\alpha\beta}(k,e)-\delta_{jl}U^{\beta\alpha}(m,i)U^{\alpha\beta}(k,e)]+\delta_{ik}\delta_{jl}\delta_{ac}\delta_{bd}[-T^\beta(m,e)]$$

$\alpha\alpha\rightarrow\alpha\alpha\alpha\beta$ $(i,j,k,l,m,a,b,c,d,e:\alpha;n,f:\beta)$

$$\langle\Psi_{ij}^{ab}|S^2|\Psi_{klmn}^{cdef}\rangle=\delta_{ik}\delta_{jl}[-\delta_{ac}\delta_{bd}U^{\alpha\beta}(m,f)U^{\beta\alpha}(n,e)+\delta_{ac}\delta_{be}U^{\alpha\beta}(m,f)U^{\beta\alpha}(n,d)-\delta_{ad}\delta_{be}U^{\alpha\beta}(m,f)U^{\beta\alpha}(n,c)]-\delta_{ik}\delta_{jm}[-\delta_{ac}\delta_{bd}U^{\alpha\beta}(l,f)U^{\beta\alpha}(n,e)$$
$$+\delta_{ac}\delta_{be}U^{\alpha\beta}(l,f)U^{\beta\alpha}(n,d)-\delta_{ad}\delta_{be}U^{\alpha\beta}(l,f)U^{\beta\alpha}(n,c)]+\delta_{il}\delta_{jm}[-\delta_{ac}\delta_{bd}U^{\alpha\beta}(k,f)U^{\beta\alpha}(n,e)+\delta_{ac}\delta_{be}U^{\alpha\beta}(k,f)U^{\beta\alpha}(n,d)$$
$$-\delta_{ad}\delta_{be}U^{\alpha\beta}(k,f)U^{\beta\alpha}(n,c)]$$

$\alpha\beta\rightarrow\alpha$ $(i,k,a,c:\alpha;j,b:\beta)$

$$\langle\Psi_{ij}^{ab}|S^2|\Psi_k^c\rangle=-\delta_{ik}U^{\alpha\beta}(a,j)U^{\beta\alpha}(b,c)+\delta_{ac}U^{\alpha\beta}(k,j)U^{\beta\alpha}(b,i)+\delta_{ik}\delta_{ac}T^\alpha(b,j)$$

$\alpha\beta\rightarrow\alpha\alpha$ $(i,k,l,a,c,d:\alpha;j,b:\beta)$

$$\langle\Psi_{ij}^{ab}|S^2|\Psi_{kl}^{cd}\rangle=-\delta_{ik}\delta_{ac}U^{\beta\alpha}(b,d)U^{\alpha\beta}(l,j)+\delta_{il}\delta_{ac}U^{\beta\alpha}(b,d)U^{\alpha\beta}(k,j)+\delta_{ik}\delta_{ad}U^{\beta\alpha}(b,c)U^{\alpha\beta}(l,j)-\delta_{il}\delta_{ad}U^{\beta\alpha}(b,c)U^{\alpha\beta}(k,j)$$

$\alpha\beta\rightarrow\alpha\beta$ $(i,k,a,c:\alpha;j,l,b,d:\beta)$

$$\langle\Psi_{ij}^{ab}|S^2|\Psi_{kl}^{cd}\rangle=-\delta_{ik}\delta_{jl}U^{\alpha\beta}(a,d)U^{\beta\alpha}(b,c)-\delta_{ac}\delta_{bd}U^{\alpha\beta}(k,j)U^{\beta\alpha}(l,i)+\delta_{ik}\delta_{bd}U^{\alpha\beta}(a,j)U_1^{\gamma x}(l,c)+\delta_{jl}\delta_{ac}U^{\alpha\beta}(k,d)U^{\beta\alpha}(b,i)$$
$$-\delta_{ik}\delta_{jl}\delta_{ac}T^\beta(b,d)+\delta_{ik}\delta_{ac}\delta_{bd}T^\beta(l,j)-\delta_{ik}\delta_{jl}\delta_{bd}T^\alpha(a,c)+\delta_{jl}\delta_{ac}\delta_{bd}T^\alpha(k,i)+\delta_{ik}\delta_{jl}\delta_{ac}\delta_{bd}\langle\Psi_0|S^2|\Psi_0\rangle$$

$\alpha\beta\rightarrow\alpha\alpha\beta$ $(i,k,l,a,c,d:\alpha;j,m,b,e:\beta)$

$$\langle\Psi_{ij}^{ab}|S^2|\Psi_{klm}^{cde}\rangle=\delta_{ik}\delta_{jm}[-\delta_{ac}U^{\beta\alpha}(b,d)U^{\alpha\beta}(l,e)+\delta_{ad}U^{\beta\alpha}(b,c)U^{\alpha\beta}(l,e)]-\delta_{il}\delta_{jm}[-\delta_{ac}U^{\beta\alpha}(b,d)U^{\alpha\beta}(k,e)$$
$$+\delta_{ad}U^{\beta\alpha}(b,c)U^{\alpha\beta}(k,e)]+\delta_{ac}\delta_{be}[\delta_{ik}U^{\beta\alpha}(m,d)U^{\alpha\beta}(l,j)+\delta_{il}U^{\beta\alpha}(m,d)U^{\alpha\beta}(k,j)]-\delta_{ad}\delta_{be}[\delta_{ik}U^{\beta\alpha}(m,c)U^{\alpha\beta}(l,j)$$
$$+\delta_{il}U^{\beta\alpha}(m,c)U^{\alpha\beta}(k,j)]-\delta_{ik}\delta_{jm}\delta_{ac}\delta_{be}[-T^\alpha(l,d)]+\delta_{il}\delta_{jm}\delta_{ac}\delta_{be}[-T^\alpha(k,d)]+\delta_{ik}\delta_{jm}\delta_{ad}\delta_{be}[-T^\alpha(l,c)]-\delta_{il}\delta_{jm}\delta_{ad}\delta_{be}[-T^\alpha(k,c)]$$

$\alpha\beta\rightarrow\alpha\alpha\beta\beta$ $(i,k,l,a,c,d:\alpha;j,m,n,b,e,f:\beta)$

$$\langle\Psi_{ij}^{ab}|S^2|\Psi_{klmn}^{cdef}\rangle=\delta_{ik}\delta_{jm}[-\delta_{ac}\delta_{be}U^{\alpha\beta}(l,f)U^{\beta\alpha}(n,d)+\delta_{ad}\delta_{be}U^{\alpha\beta}(l,f)U^{\beta\alpha}(n,c)+\delta_{ac}\delta_{bf}U^{\alpha\beta}(l,e)U^{\beta\alpha}(n,d)-\delta_{ad}\delta_{bf}U^{\alpha\beta}(l,e)U^{\beta\alpha}(n,c)]$$
$$-\delta_{il}\delta_{jm}[-\delta_{ac}\delta_{be}U^{\alpha\beta}(k,f)U^{\beta\alpha}(n,d)+\delta_{ad}\delta_{be}U^{\alpha\beta}(k,f)U^{\beta\alpha}(n,c)+\delta_{ac}\delta_{bf}U^{\alpha\beta}(k,e)U^{\beta\alpha}(n,d)-\delta_{ad}\delta_{bf}U^{\alpha\beta}(k,e)U^{\beta\alpha}(n,c)]$$
$$-\delta_{ik}\delta_{jn}[-\delta_{ac}\delta_{be}U^{\alpha\beta}(l,f)U^{\beta\alpha}(m,d)+\delta_{ad}\delta_{be}U^{\alpha\beta}(l,f)U^{\beta\alpha}(m,c)+\delta_{ac}\delta_{bf}U^{\alpha\beta}(l,e)U^{\beta\alpha}(m,d)-\delta_{ad}\delta_{bf}U^{\alpha\beta}(l,e)U^{\beta\alpha}(m,c)]$$
$$+\delta_{il}\delta_{jn}[-\delta_{ac}\delta_{be}U^{\alpha\beta}(k,f)U^{\beta\alpha}(m,d)+\delta_{ad}\delta_{be}U^{\alpha\beta}(k,f)U^{\beta\alpha}(m,c)+\delta_{ac}\delta_{bf}U^{\alpha\beta}(k,e)U^{\beta\alpha}(m,d)-\delta_{ad}\delta_{bf}U^{\alpha\beta}(k,e)U^{\beta\alpha}(m,c)]$$

[a] $T^\alpha(p,q)=\sum_i^{\text{occ}} S_{\tilde{i}p}S_{q\tilde{i}}$, $T^\beta(p,q)=\sum_i^{\text{occ}} S_{i\tilde{p}}S_{\tilde{q}i}$, $U^{\alpha\beta}(p,q)=S_{p\tilde{q}}=\int\phi_p s_+\tilde{\phi}_q d\tau$, $U^{\beta\alpha}(p,q)=S_{\tilde{p}q}=\int\tilde{\phi}_p s_-\phi_q d\tau$.

$$\langle S^2\rangle=\langle\Psi_0|S^2|\Psi\rangle+\left\langle\Psi_0|\mathbf{H}|\frac{d\Psi_{\rm corr}}{d\lambda}\Big|_{\lambda=0}\right\rangle \tag{10}$$

with the restriction that the orbitals of reference state do not change with the external perturbation term λS^2. First-order perturbation theory can be used to estimate $d\Psi_{\rm corr}/d\lambda$:

$$\langle\Psi_s|\mathbf{H}+\lambda S^2|\Psi+\delta\Psi(\lambda)\rangle=[E+\delta E(\lambda)]\langle\Psi_s|\Psi+\delta\Psi(\lambda)\rangle,$$
$$\delta E(\lambda)=\lambda\langle S^2\rangle. \tag{11}$$

By making the approximation

$$\langle\Psi_t|\mathbf{H}-E|\delta\Psi_{\rm corr}\rangle=(E_t-E_0)\langle\Psi_t|\delta\Psi_{\rm corr}\rangle\quad(t=S,D), \tag{12}$$

the expression of $\langle S^2\rangle$ can be written as

$$\langle S^2\rangle=\{\langle\Psi_0|S^2|\Psi\rangle+\delta_1+\delta_2\}/(1+\delta_d)$$
$$\delta_d=-\sum\langle\Psi_0|\mathbf{H}|\Psi_{ij}^{ab}\rangle\langle\Psi_{ij}^{ab}|\Psi\rangle/\Delta_{ij}^{ab},$$
$$\delta_1=-\sum\langle\Psi_0|\mathbf{H}|\Psi_i^a\rangle\langle\Psi_i^a|S^2|\Psi\rangle/\Delta_i^a \tag{13}$$
$$\delta_2=-\sum\langle\Psi_0|\mathbf{H}|\Psi_{ij}^{ab}\rangle\langle\Psi_{ij}^{ab}|S^2|\Psi\rangle/\Delta_{ij}^{ab}$$

where $\Delta_a^i=\epsilon_a-\epsilon_i$ and $\Delta_{ij}^{ab}=\epsilon_a+\epsilon_b-\epsilon_i-\epsilon_j$ (the ϵ's are orbital energies). Because of Brillouin's theorem, δ_1 is zero for UCI, UCC, and UQCI methods; however in the UBD approach, this term is nonzero. Note that if the first-order perturbation wave function is substituted for $\Psi_{\rm corr}$, the value of $\langle S^2\rangle_{\rm MP2}$ is obtained by omitting the higher order contributions. In this paper all values for $\langle S^2\rangle$ for CID, CISD, CCD, CCSD, QCISD, and BD are calculated by using Eq. (13).

An expression for $\langle S^2\rangle$ that is more like the perturbation theory results can be obtained by expanding the denominator of Eq. (13) and collecting terms up to the first order,

$$\langle S^2\rangle=\langle\Psi_0|S^2|\Psi\rangle+\langle\Psi_0|\mathbf{H}|\Psi_i^a\rangle\delta_i^a+\langle\Psi_0|\mathbf{H}|\Psi_{ij}^{ab}\rangle\delta_{ij}^{ab}$$
$$\delta_i^a=-\langle\Psi_i^a|S^2|\Psi\rangle/\Delta_i^a, \tag{14}$$
$$\delta_{ij}^{ab}=-\langle\Psi_{ij}^{ab}|(S^2-\langle S^2\rangle_0)|\Psi\rangle/\Delta_{ij}^{ab}.$$

As mentioned above, the QCISD method does not have a well-defined wave function, but an approximation to the wave function is required to compute $\langle S^2\rangle_{\rm QCISD}$. Either $\Psi=(1+\mathbf{T}_1+\mathbf{T}_2+\frac{1}{2}\mathbf{T}_2^2)\Psi_0$ or $\Psi=(1+\mathbf{T}_1+\mathbf{T}_2+\mathbf{T}_1\mathbf{T}_2+\frac{1}{2}\mathbf{T}_2^2)\Psi_0$ can be used in Eq. (13). As will be seen below the two choices give almost the same numerical values for $\langle S^2\rangle$.

Similar to S^2 for UMPn, the matrix elements $\langle\Psi_0|S^2|\Psi_u\rangle$ ($u=S$, D) and $\langle\Psi_D|S^2|\Psi_u\rangle$ ($u=S$, D, T, and Q) are required to compute S^2 for UCI, UCC, UQCI, and UBD. Since the triple excitations can be expressed as $\mathbf{T}_1\mathbf{T}_2\Psi_0$, the calculation of $\langle\Psi_0|\mathbf{H}|\Psi_{ij}^{ab}\rangle\langle\Psi_{ij}^{ab}|S^2|\mathbf{T}_1\mathbf{T}_2\Psi_0\rangle$ requires only $O(N^6)$ steps. The total computational cost of $\langle S^2\rangle$ is about one-third of the cost of one UCCSD iteration which involves 15 $O(N^6)$ order steps.[20]

SPIN PROJECTION OF UMPn ENERGIES

The equations for the projected Hartree–Fock energy are well known and can be written in terms of the Löwdin spin projection operator[15] $\mathbf{P}_s$:

$$\begin{cases}E_{\rm proj\ UHF}=\langle\Psi_0|\mathbf{H}\mathbf{P}_s|\Psi_0\rangle/\langle\Psi_0|\mathbf{P}_s|\Psi_0\rangle\\ \mathbf{P}_s=\prod_{k\neq s}\{[S^2-k(k+1)]/[s(s+1)-k(k+1)]\}.\end{cases} \tag{15}$$

Note that $\mathbf{P}_s$ is idempotent and commutes with $\mathbf{H}$ since the Hamiltonian is spin free. Often the largest contribution to the spin contamination in MPn calculation comes from the next highest spin multiplicity.[17] Under such circumstances the full spin projection operator can be approximated quite well by an operator $\mathbf{A}_{s+1}$ that annihilates only the next highest spin, $\mathbf{A}_{s+1}=[S^2-(s+2)(s+1)]/[\langle S^2\rangle_0-(s+2)(s+1)]$.

For Møller–Plesset perturbation theory, full spin projection would apply the projector to the correlation corrections as well as Ψ_0. One way of writing projected energies for UMPn wave functions is[19]

$$E_{\rm proj\ MPn}=\frac{\langle\Psi_0|\mathbf{H}\mathbf{P}_s|\Psi_0+\Psi_1+\cdots+\Psi_{n-1}\rangle}{\langle\Psi_0|\mathbf{P}_s|\Psi_0+\Psi_1+\cdots+\Psi_{n-1}\rangle}. \tag{16}$$

If the identity $I=\Sigma_i|\Psi_i\rangle\langle\Psi_i|$ is inserted into Eq. (16), the spin projected energies can be written as

$$E_{\rm proj\ MPn}=\langle\Psi_0|\mathbf{H}|\Psi_0\rangle+\sum_i\frac{\langle\Psi_0|\mathbf{H}|\Psi_i\rangle\langle\Psi_i|\mathbf{P}_s|\Psi_0+\Psi_1+\cdots+\Psi_{n-1}\rangle}{\langle\Psi_0|\mathbf{P}_s|\Psi_0+\Psi_1+\cdots+\Psi_{n-1}\rangle}. \tag{17}$$

Alternatively, if $\mathbf{H}$ and $\mathbf{P}_s$ in Eq. (16) are commuted, the spin projected energies are

$$E_{\rm proj\ MPn}=\frac{\langle\Psi_0|\mathbf{P}_s|\Psi_0\rangle\langle\Psi_0|\mathbf{H}|\Psi_0+\cdots+\Psi_{n-1}\rangle+\Sigma_i\langle\Psi_0|\mathbf{P}_s|\Psi_i\rangle\langle\Psi_i|\mathbf{H}|\Psi_0+\cdots+\Psi_{n-1}\rangle}{\langle\Psi_0|\mathbf{P}_s|\Psi_0+\cdots+\Psi_{n-1}\rangle}. \tag{18}$$

If $\mathbf{P}_s$ is approximated by $\mathbf{A}_{s+1}$, then Ψ_i in Eq. (18) need only include all single and double excitations.

Equation (18) has been implemented previously in the Gaussian computational package at the UMP2 level.[19] The advantage of using Eq. (18) is that only matrix elements of the type $\langle\Psi_0|S^2|\Psi_u\rangle$ ($u=S$, D) are used, while the disadvantage is that the computation of $\langle\Psi_i|\mathbf{H}|\Psi_{n-1}\rangle$ is almost as much work as computing Ψ_n or E_{n+1} [this limits practical implementation of Eq. (18) to the third order]. On the other hand, Eq. (17) uses only Ψ_{n-1} to calculate the projected nth-order perturbation energy but it requires the calculation of matrix elements of $\langle\Psi_D|S^2|\Psi_u\rangle$ ($u=S$, D, T, and Q). The

TABLE II. Values of $\langle S^2 \rangle$ for HF→H+F.

R(Å)	SCF	MP2	MP4	CID	CISD	CCD	CCSD	QCISD Without T_1T_2	QCISD With T_1T_2	BD
1.2764[a]	0.0000	0.0000	0.0000	0.0000	0.0000	0.0000	0.0000	0.0000	0.0000	0.0000
1.4	0.3852	0.3282	0.1280	0.3030	0.1085	0.2973	0.0112	0.0108	0.0071	0.0000
1.6	0.7098	0.6575	0.4807	0.5980	0.3147	0.5808	0.0573	0.0603	0.0558	0.0000
1.8	0.8590	0.8264	0.7219	0.7599	0.5411	0.7295	0.1687	0.1702	0.1670	0.0000
2.0	0.9307	0.9122	0.8560	0.8566	0.7334	0.8159	0.3670	0.3607	0.3591	0.0013
2.1	0.9513	0.9376	0.8970	0.8904	0.8042	0.8473	0.4872	0.4782	0.4772	0.3358
2.2	0.9659	0.9557	0.9265	0.9171	0.8583	0.8741	0.6045	0.5953	0.5947	0.5524
2.4	0.9835	0.9778	0.9628	0.9543	0.9278	0.9177	0.7880	0.7828	0.7826	0.7804
2.6	0.9923	0.9890	0.9813	0.9759	0.9639	0.9502	0.8938	0.8917	0.8916	0.8927
2.8	0.9967	0.9947	0.9907	0.9877	0.9823	0.9721	0.9481	0.9473	0.9473	0.9481
3.0	0.9989	0.9975	0.9954	0.9940	0.9915	0.9854	0.9751	0.9748	0.9748	0.9755
3.2	1.0000	0.9989	0.9977	0.9972	0.9960	0.9928	0.9883	0.9882	0.9882	0.9887
3.4	1.0005	0.9996	0.9988	0.9987	0.9982	0.9967	0.9947	0.9946	0.9946	0.9949

[a]Onset of the UHF-RHF instability.

results presented in this paper utilize Eq. (17). It should be emphasized that Eqs. (17) and (18) are identical only for full-core calculations. If frozen-core calculations are performed, $I=\Sigma_i|\Psi_i\rangle\langle\Psi_i|$ is no longer the identity operator. The test results show the differences between Eqs. (17) and (18) are a few millihartree for frozen-core calculations of projected UMP3 energies.

The matrix elements needed for projected UMP2 and UMP3 methods by using Eq. (17) are similar to those for the calculation of $\langle S^2 \rangle$ for CCSD. The projected UMP4(SDTQ) energy requires the coefficients of singles, doubles, triples, and quadruples excitations of Ψ_3. Since these require up to $O(N^7)$ work and $O(N^8)$ storage, we have omitted these two components. As discussed below, comparisons with projection calculations using the full CI code (which include these terms) shows that this is a reasonable approximation in the region where the contributions from the triple and quadruple excitations of the third-order correction are not large. Since the spin projected correction for the fourth-order energy E_4 is usually not very large, the following less expensive approach may also be used to estimated the spin projected UMP4(SDTQ) energy

$$E_{\text{proj MP4}} \approx E_{\text{proj MP3}} + E_4(\text{SDTQ})$$
$$= \langle\Psi_0|\mathbf{H}|\Psi_i\rangle + \sum_i \frac{\langle\Psi_0|\mathbf{H}|\Psi_i\rangle\langle\Psi_i|\mathbf{P}_s|\Psi_0+\Psi_1+\Psi_2\rangle}{\langle\Psi_0|\mathbf{P}_s|\Psi_0+\Psi_1+\Psi_2\rangle} + E_4(\text{SDTQ}). \quad (19)$$

RESULTS AND DISCUSSION

The formulas for $\langle S^2 \rangle$ and projected unrestricted Møller–Plesset perturbation theory presented above have been implemented in the development version of the GAUSSIAN program[10] and tested against the full configuration interaction (FCI) code. Equation (13) was used to calculate $\langle S^2 \rangle$ for UCC, UQCI, and UBD methods; Eq. (5) was used for UMPn. Projected UMPn energies were computed according to Eq. (17). The spin projection operator $\mathbf{P}_s$ was approximated by the single annihilation operator $\mathbf{A}_{s+1}$ which removes only the next highest spin contaminant. The projected UMP4 energy does not include the contributions from triple and quadruple excitations of the third-order correlation correction to the wave function; an approximate approach based on projected MPn according to Eq. (19) was also tested.

To demonstrate the evaluation of S^2 and projected energies, the single bond dissociation potential curves of HF→H+F and CH_4→CH_3+H have been calculated with the MP4, CCSD, QCISD, and BD methods. These calculations may also be relevant for transition states, since many contain partially broken bonds. All the calculations used all core, valence, and unoccupied orbitals with the 6-31G basis set for HF and the 6-31G** basis set for CH_4. Full CI calculations were been performed with the 6-31G basis set for HF dissociation for the comparison with the various levels of theory. The full CI code was also used to evaluate the full spin projected UMP4 energies according to Eq. (16) for comparison with Eqs. (17) and (19). To eliminate the effects from other modes in the CH_4 system, the stretching coordinates calculated by Hirst[21] were used.

Table II lists the values of S^2 for the UMP2, UMP4(SDTQ), UCID, UCISD, UCCD, UCCSD, UQCISD, and UBD methods at different hydrogen fluoride bond lengths; Table III gives similar data for methane. Since the QCISD wave function is not well-defined, S^2 computed with and without the T_1T_2 Ψ_0 term in the QCISD wave function. The differences between these two approaches are no larger than 0.005, and either could be used to represent S^2 of a QCISD calculation. All the post-SCF methods discussed here (UMPn, UCC, UQCI, and UBD) have smaller values of S^2 than the Hartree–Fock wave function at the same bond length. This is expected since S^2 for the exact ground state wave function is zero and the correlated wave functions are closer to the exact wave function than the UHF wave function. For all the unrestricted methods, S^2 tend toward 1.0 as the bond dissociates. For a two electron two orbital system, if the orbitals are well separated and there is no interaction between the electrons, the unrestricted Hartree–Fock wave function contains an equal mixture of singlet ($s=0$) and

TABLE III. Values of $\langle S^2 \rangle$ for $CH_4 \rightarrow CH_3+H$.

								QCISD		
R(Å)	SCF	MP2	MP4	CID	CISD	CCD	CCSD	Without T_1T_2	With T_1T_2	BD
1.50	0.0000	0.0000	0.0000	0.0000	0.0000	0.0000	0.0000	0.0000	0.0000	0.0000
1.75	0.2275	0.2303	0.0873	0.2166	0.1318	0.2074	0.0198	0.0246	0.0192	0.0000
2.00	0.6591	0.6001	0.4408	0.5590	0.4223	0.5291	0.1275	0.1302	0.1401	0.0000
2.25	0.8395	0.7986	0.6993	0.7552	0.6772	0.7110	0.3440	0.3550	0.3490	0.0004
2.50	0.9269	0.9008	0.8448	0.8686	0.8310	0.8222	0.6050	0.6106	0.6081	0.5171
2.75	0.9699	0.9525	0.9212	0.9328	0.9156	0.8948	0.7960	0.7993	0.7984	0.7796
3.00	0.9911	0.9785	0.9600	0.9675	0.9593	0.9419	0.9005	0.9026	0.9022	0.8973
4.00	1.0103	1.0022	0.9960	1.0015	0.9997	0.9993	0.9961	0.9963	0.9962	0.9962

triplet ($s=1$) states; hence, the average value of S^2 should be 1.0. The UHF values of S^2 for both hydrogen fluoride and methane are slightly larger than 1.0 at large bond lengths, indicating that the UHF wave function contains small contributions from higher spin states ($s>1$). The values of S^2 for the post-SCF methods are all less than 1.0.

Figure 1 shows the changes in S^2 with respect to bond length in hydrogen fluoride and methane. It is readily apparent that iterative calculations (UCI, UCC, and UQCI) reduce the spin contamination much more than noniterative methods (UMPn); furthermore, the coupled cluster and quadratic configuration interaction methods clean up the spin contamination better than the truncated configuration interaction method. In particular, the order of the values of S^2 is UCCSD≅UQCISD<UCISD<UMP4<UMP2<UHF at all bond lengths. This ordering is in agreement with the generally accepted ranking of the accuracy of these wave functions. The UQCISD and UCCSD curves in Fig. 1 are nearly identical, showing that both methods have very similar behavior with respect to spin. This result supports a statement made by Pople[22] that the CCSD and QCISD calculations are very similar in quality.

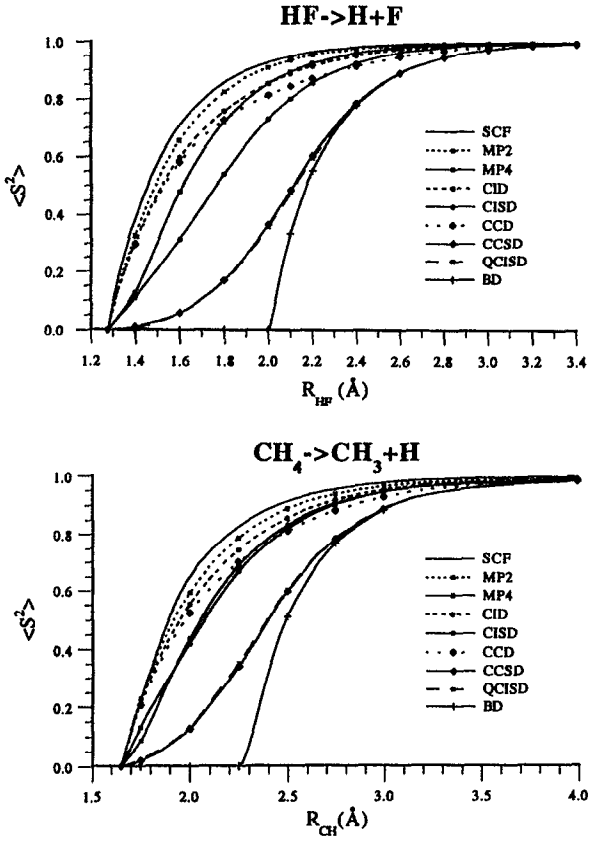

FIG. 1. Values of S^2 as a function of bond length for HF→H+F and $CH_4 \rightarrow CH_3+H$.

The values of the S^2 for CISD and CCSD theories are smaller than those for CID and CCD, indicating that the CISD and CCSD wave functions have less spin contamination than the CID and CCD wave functions. Table IV lists matrix elements $\langle \Psi_0|S^2|\Psi_0\rangle$, $\langle \Psi_0|S^2|\Psi_S\rangle$, and $\langle \Psi_0|S^2|\Psi_D\rangle$, which are the main contributors to S^2 for CCD and CCSD. As expected, near the onset of the UHF-RHF instability, the contributions from the single substitutions are larger than from the double substitutions. However, a few tenths of an angstrom beyond the instability, the $\langle \Psi_0|S^2|\Psi_D\rangle$ term dominates. The absolute value of $\langle \Psi_0|S^2|\Psi_D\rangle$ for UCCSD is two to four times greater than that for UCCD. Thus at long bond lengths, the primary effect of the single substitutions is to reduce S^2 by increasing the contributions from Ψ_D ($\langle \Psi_0|S^2|\Psi_D\rangle$) rather than reducing S^2 directly through contributions from $\langle \Psi_0|S^2|\Psi_S\rangle$.

Handy and Pople[5] have pointed out that the restricted Brueckner doubles method is stable with respect to spin-unrestricted displacements over a wider range of nuclear ge-

TABLE IV. Matrix elements of $\langle \Psi_0|S^2|\Psi_0\rangle$, $\langle \Psi_0|S^2|\Psi_S\rangle$, and $\langle \Psi_0|S^2|\Psi_D\rangle$ for UCCD and UCCSD calculations on HF→H+F.

		UCCD	UCCSD	
R(Å)	$\langle \Psi_0\|S^2\|\Psi_0\rangle$	$\langle \Psi_0\|S^2\|\Psi_D\rangle$	$\langle \Psi_0\|S^2\|\Psi_S\rangle$	$\langle \Psi_0\|S^2\|\Psi_D\rangle$
1.4	0.385 19	−0.059 89	−0.249 45	−0.123 86
1.6	0.709 76	−0.103 13	−0.293 20	−0.357 29
1.8	0.858 99	−0.113 62	−0.195 28	−0.491 76
2.0	0.930 65	−0.106 07	−0.095 32	−0.464 81
2.2	0.965 90	−0.087 29	−0.036 22	−0.322 49
2.4	0.983 46	−0.063 43	−0.012 19	−0.181 60
2.6	0.992 26	−0.040 91	−0.004 19	−0.093 41
2.8	0.996 67	−0.023 94	−0.001 59	−0.046 53
3.0	0.998 87	−0.013 13	−0.000 67	−0.022 87
3.2	0.999 95	−0.006 97	−0.000 33	−0.011 20
3.4	1.000 48	−0.003 73	−0.000 19	−0.005 54

TABLE V. Differences in $\langle S^2 \rangle$ for HF→H+F computed using Eqs. (13) and (20).[a]

					QCISD		
R(Å)	CID	CISD	CCD	CCSD	Without T_1T_2	With T_1T_2	BD
1.4	0.0274	0.0067	0.0280	0.0007	−0.0032	0.0005	
1.6	0.0249	0.0101	0.0258	0.0020	−0.0023	0.0022	
1.8	0.0172	0.0086	0.0159	0.0033	0.0003	0.0035	
2.0	0.0082	0.0057	0.0087	0.0036	0.0020	0.0036	−0.0006
2.1	0.0059	0.0043	0.0063	0.0032	0.0022	0.0033	−0.0772
2.2	0.0043	0.0032	0.0045	0.0027	0.0021	0.0027	−0.0513
2.4	0.0021	0.0017	0.0023	0.0017	0.0014	0.0016	−0.0143
2.6	0.0011	0.0009	0.0011	0.0009	0.0008	0.0009	−0.0043
2.8	0.0006	0.0005	0.0006	0.0004	0.0004	0.0004	−0.0015
3.0	0.0003	0.0002	0.0003	0.0002	0.0002	0.0002	−0.0006
3.2	0.0002	0.0001	0.0002	0.0001	0.0001	0.0001	−0.0002
3.4	0.0001	0.0000	0.0001	0.0000	0.0000	0.0001	−0.0001

[a]Equation (20) minus Eq. (13).

ometries than Hartree–Fock theory. The onset of the UBD-RBD instability is at ~2 Å for hydrogen fluoride with the 6-31G basis set, while the onset of UHF-RHF instability is at 1.2764 Å. From Fig. 1, the UBD curves for both HF and CH_4 have large slopes initially and then merge with the UCCSD and UQCISD curves. The similar behavior in S^2 a few tenths of an Angstrom beyond the onset of UBD-RBD instability may explain why UQCISD, UCCSD, and UBD give comparable results for the single bond dissociation potential curves. For both systems, S^2 for UQCISD and UCCSD is about 0.35 at the onset of the UBD-RBD instability. This could be quite useful in predicting the onset of the UBD-RBD instability for single bond dissociations.

Bartlett and co-workers[23] have computed S^2 for coupled cluster wave functions using

$$\langle S^2 \rangle_B = \langle \Psi_0 | S^2 | \Psi \rangle. \tag{20}$$

Unlike Eqs. (13) and (14), this expression does not consider contributions from the change in the wave function arising from the spin perturbation. Table V list the differences in the values of S^2 computed by Eqs. (20) and (13) at various levels of the theory for hydrogen fluoride, showing that the two approaches give almost the same results. The differences are generally less than 0.01 at distances greater than 1.8 Å for all the levels of theory except UBD. For UBD, the differences are very small when R_{HF} is larger than 2.4 Å. The relative differences (compare Tables II and V) are a few percent or less except for UBD for which the differences reach about 20% just beyond the onset of UBD-RBD instability. This indicates that the Hellmann–Feynman theorem is approximately satisfied for UCISD, UCISD, and UQCISD wave functions for perturbations involving spin for these cases. Similar results are found for the CH_4 system. Although the second and third terms and denominator in Eqs. (13) and (14) are not small individually for the examples presented here, they cancel.

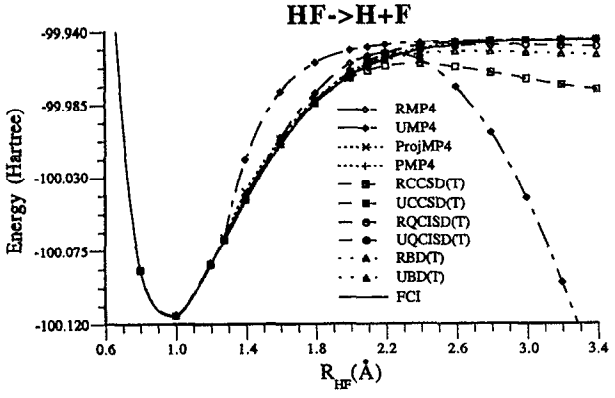

FIG. 2. Potential energy curves for HF→H+F at various levels of theory.

Figure 2 shows a number of potential energy curves for HF computed at various levels of theory. The RMP4 calculations give the wrong limit as the HF bond dissociates, while UMP4 goes to the correct limit but shows convergence problems at intermediate bond lengths. These two features are well known. The maximum energy difference between UMP4 and full CI is 33 mhartree at the bond length of ~1.6 Å. The values of S^2 at $R_{HF}=1.6$ Å are 0.71 for UHF and 0.48 for UMP4. In the region where the value of S^2 is about 0.5 for the UMP4 calculation, the higher order perturbation corrections to the energy play an important role. This is the recoupling region where the wave function changes character from a pair of singlet coupled electrons to a pair of uncoupled electrons. The iterative methods for the electron correlation correction (CCSD, QCISD, and BD) give much better results for the energy in the recoupling region than the noniterative method (MP4), similar to the calculations of S^2. All the unrestricted methods used in Fig. 2 reach the correct limit, while the restricted methods give incorrect results when the molecule dissociates.

Table VI lists the differences between projected MP4 and full CI energies. For practical reasons, two approximations need to be made for calculations on larger molecules: (a) the single annihilator $\mathbf{A}_{s+1}$ is used instead of full projector $\mathbf{P}_s$ and (b) the triples and quadruples contributions to the third-order wave function ($\Psi_{3T,Q}$) are neglected in computing the projected MP4 energy using Eq. (17). For comparison, Table VI also lists the projected MP4 energies including these terms (computed with the full CI code), the projected

TABLE VI. Energy differences (in hartree) between MP4 and full CI calculations for HF→H+F.[a,b]

			UMP4 with single annihilation		UMP4 with full projection	
R(Å)	RMP4	UMP4	Eq. (17) without $\Psi_{3T,Q}$	Eq. (19)	Eq. (17) with $\Psi_{3T,Q}$	Eq. (16)
1.4	0.002 617	0.025 722	0.007 911	0.002 094	0.005 588	0.005 577
1.6	0.004 573	0.033 031	0.006 301	0.002 494	0.003 773	0.003 793
1.8	0.006 702	0.024 980	0.004 298	0.002 564	0.002 551	0.002 620
2.0	0.007 410	0.015 604	0.002 766	0.001 942	0.001 729	0.001 836
2.1	0.006 443	0.011 866	0.002 154	0.001 546	0.001 379	0.001 498
2.2	0.004 119	0.008 887	0.001 655	0.001 181	0.001 082	0.001 211
2.4	−0.005 973	0.004 872	0.000 964	0.000 628	0.000 659	0.000 800
2.6	−0.025 194	0.002 680	0.000 584	0.000 307	0.000 424	0.000 571
2.8	−0.055 070	0.001 541	0.000 390	0.000 139	0.000 305	0.000 455
3.0	−0.096 245	0.000 966	0.000 294	0.000 055	0.000 247	0.000 399
3.2	−0.148 515	0.000 682	0.000 248	0.000 016	0.000 220	0.000 373
3.4	−0.210 912	0.000 545	0.000 226	−0.000 003	0.000 208	0.000 361

MP4 energies calculated by the approximation in Eq. (19), and the MP4 energies computed with the full projector. The differences between single annihilation and full projections are very small for HF dissociation and are generally negligible for most single bond breaking cases. However, the error from neglecting the Ψ_{3T} and Ψ_{3Q} terms is significant in the recoupling region. The maximum error is about 2.5 mhartree and occurs at a bond length of ~1.6 Å, which is near the maximum in the difference between the UMP4 and full CI energies. Although the triple and quadruple excitation terms in Ψ_3 do not contribute to the UMP4 energy, they do contribute to the projected energy and speed up the convergence of the projected UMPn calculations. For $R_{HF}>1.8$ Å, these terms are almost negligible.

The approximation to spin projected MP4 energy given by Eq. (19) assumes that the spin contamination in Ψ_3 can be neglected. In our previous papers,[17,19] this approximation was necessary for practical reasons, but appeared to work quite well. The energies calculated by Eq. (19) are overestimated when compared with the fully projected MP4 energy from Eq. (16), but the overestimation seems to cancel some of the higher order corrections. This method appears to be quite effective and practical for a single bond dissociation system, since it gives very good results when compared with the full CI calculation and its additional cost is negligible compared with the UMP4(SDTQ) calculation.

TABLE VII. Energy differences (in hartree) between single annihilation and full projection for HF→H+F.

R(Å)	ΔE_{SCF}	ΔE_{MP2}	ΔE_{MP3}	ΔE_{MP4}
1.4	−0.000 1347	−0.000 0608	−0.000 0128	−0.000 0105
1.6	−0.000 4765	−0.000 2397	−0.000 0946	−0.000 0199
1.8	−0.000 7088	−0.000 3760	−0.000 1774	−0.000 0697
2.0	−0.000 8342	−0.000 4553	−0.000 2322	−0.000 1068
2.1	−0.000 8713	−0.000 4798	−0.000 2502	−0.000 1194
2.2	−0.000 8974	−0.000 4974	−0.000 2635	−0.000 1289
2.4	−0.000 9288	−0.000 5191	−0.000 2802	−0.000 1410
2.6	−0.000 9446	−0.000 5303	−0.000 2890	−0.000 1473
2.8	−0.000 9528	−0.000 5361	−0.000 2936	−0.000 1505
3.0	−0.000 9572	−0.000 5391	−0.000 2960	−0.000 1522
3.2	−0.000 9595	−0.000 5407	−0.000 2972	−0.000 1531
3.4	−0.000 9608	−0.000 5416	−0.000 2978	−0.000 1535

Tables VII and VIII list the differences between single annihilated and fully projected energies for breaking one bond in HF and two bonds in H_2O. Three important features can be observed: (a) the single annihilated energies are lower than fully projected energies for any order of the perturbation theory (this was first pointed out by Morokuma and co-workers[24]); (b) the higher the order of perturbation calculation used, the smaller the difference between single annihilation and full projection; (c) the difference between single annihilation and full projection for any order of the wave function increases with increasing bond lengths and tends toward a constant. For breaking one bond in HF, the error in MP3 and MP4 energies with single annihilation are at least three and six times smaller than for the UHF calculations, respectively. For breaking two bonds in H_2O, a reduction in the error with higher order MPn calculation is also observed, although the error with higher order perturbation calculations are still very large when only single annihilation is used. However, annihilation of two spin contaminants gives results that are in very good agreement with full projection, especially with higher order perturbation theory (Table VIII). The higher order UMPn calculations tend to reduce the weight of the configurations contaminating the UHF wave function. Morokuma[24] used an approximate method[17] which projected out the spin contamination from the UHF wave function but not the UMPn wave function; hence the effect of projected higher order UMPn was not evident.

Figure 3 shows the differences between the CCSD(T), QCISD(T), BD(T), and full CI energies for HF or MRDCI energies[21] for CH_4. In the two regions where hydrogen fluoride is either well bonded or well separated, the restricted and unrestricted CCSD(T), QCISD(T), and BD(T) methods are in very good agreement with the full CI calculations, respectively. The energy differences are only a few tenths of millihartrees in these two limits. In the region between the onsets of the UHF-RHF and UBD-RBD instabilities, restricted and unrestricted CCSD(T), QCISD(T), and BD(T) have about the same errors when compared with the full CI calculation. The largest errors in this region are ~0.6, 1.5,

TABLE VIII. Energy differences (in hartree) between single annihilation, double annihilation, and full projection for $H_2O \rightarrow 2H+O$.

R(Å)	Annihilation	ΔE_{SCF}	ΔE_{MP2}	ΔE_{MP3}	ΔE_{MP4}	ΔE_{MP5}
1.425	single	−0.026 297	−0.023 979	−0.013 596	−0.008 210	0.003 940
	double	0.000 143	0.000 058	−0.000 003	−0.000 029	−0.000 038
1.9	single	−0.172 142	−0.156 831	−0.120 308	−0.103 502	−0.089 074
	double	0.002 021	0.001 122	0.000 533	0.000 197	0.000 022
2.85	single	−0.886 427	−0.471 182	−0.281 200	−0.197 682	−0.153 676
	double	0.003 123	0.001 860	0.001 067	0.000 573	0.000 308

0.9, 0.8, and 1.0 mhartree for RCCSD(T), UCCSD(T), RQCISD(T), UQCISD(T), and RBD(T), respectively. The maximum errors in the UCCSD(T), UQCISD(T), and UBD(T) curves are ~3.5 mhartree and occur at ~2.2 Å, about 0.2 Å beyond the onset of the UBD-RBD instability. The values of S^2 at these maxima are 0.5–0.6 (for UMP4, S^2 is also ~0.5, but the maximum error in the energy occurs at ~1.6 Å. For comparison, the error curve for the approximate projected MP4 calculated by Eq. (19) is also plotted in Fig. 3. In the region where the UCCSD(T), UQCISD(T), and UBD(T) errors are large, the error in the projected MP4 energy is small; conversely, CCSD(T), QCISD(T) and BD(T) are in very good agreement with the full CI energies where error in the projected MP4 is large. The results for CH_4 are similar. We estimate that the MRD-CI calculations of Hirst[21] are about 3 mhartree above the full CI calculations.

Figure 4 shows the errors in energy for restricted and unrestricted CCSD, QCISD, and BD methods with and without the noniterative triples correction. In the unrestricted approach, the triple substitutions play a very important role in adjusting the incorrect behavior remaining in the wave functions in the recoupling region. This correction becomes less important at large bond lengths where the character of the pair of uncoupled electrons is well established. On the other hand, the restricted calculations without triples tend toward a higher limit in energy when the molecule dissociates. This result is expected because in the dissociation limit the restricted Hartree–Fock wave function is a mixture of ionic ($H^+ + F^-$) and diradical ($H^{\cdot} + F^{\cdot}$) configurations. To remove the ionic contribution, the restricted wave functions must have large amplitudes for the single and double substitutions. Hence the triple substitutions produce a large correction to

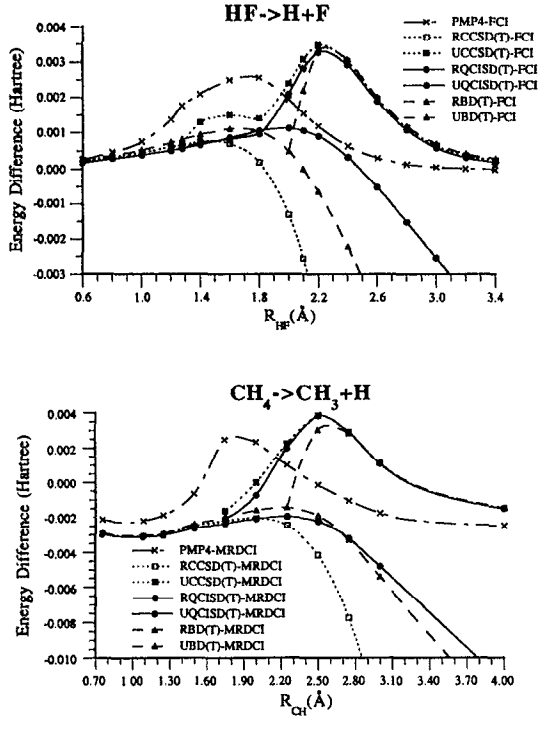

FIG. 3. Energy differences between various levels of theory and full CI energies for $HF \rightarrow H+F$, and MRDCI energies for $CH_4 \rightarrow CH_3+H$.

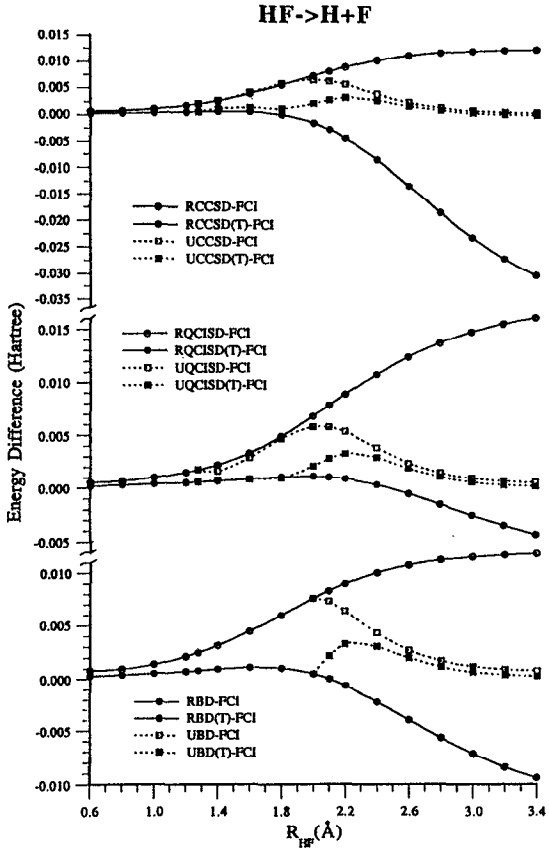

FIG. 4. Energy differences between restricted and unrestricted coupled clusters, quadratic CI, Brueckner doubles with and without triples correction, and full CI for $HF \rightarrow H+F$.

TABLE IX. Triples contribution to the correlation energy ΔE_T (in mhartree) and normalization factor A_{norm} for HF→H+F.

	RCCSD		UCCSD		RQCISD		UQCISD		RBD		UBD	
R(Å)	ΔE_T	A_{norm}	ΔE_T	A_{norm}	ΔE_T	A_{norm}	ΔE_T	A_{norm}	ΔE_T	A_{norm}	ΔE_T	A_{norm}
0.6	−0.464	1.0121			−0.363	1.0122			−0.533	1.0120		
0.8	−0.500	1.0145			−0.396	1.0146			−0.571	1.0144		
1.0	−0.763	1.0185			−0.605	1.0186			−0.871	1.0181		
1.2	−1.251	1.0257			−0.973	1.0258			−1.408	1.0246		
1.2764	−1.510	1.0299	−1.510	1.0299	−1.163	1.0300	−1.163	1.0300	−1.677	1.0282		
1.4	−2.048	1.0390	−1.512	1.1073	−1.548	1.0391	−0.880	1.1267	−2.205	1.0360		
1.6	−3.375	1.0626	−2.786	1.1829	−2.453	1.0619	−2.067	1.2231	−3.360	1.0553		
1.8	−5.552	1.1009	−4.534	1.1969	−3.823	1.0975	−3.707	1.2328	−4.992	1.0849		
2.0	−8.866	1.1554	−4.333	1.1457	−5.698	1.1457	−3.694	1.1648	−7.136	1.1245	−7.127	1.1244
2.1	−10.978	1.1875	−3.412	1.1066	−6.798	1.1731	−2.952	1.1185	−8.366	1.1469	−5.171	1.1005
2.2	−13.366	1.2216	−2.405	1.0711	−7.977	1.2014	−2.090	1.0778	−9.662	1.1701	−3.135	1.0659
2.4	−18.762	1.2910	−1.085	1.0289	−10.462	1.2575	−0.914	1.0305	−12.305	1.2157	−1.267	1.0270
2.6	−24.528	1.3555	−0.626	1.0151	−12.940	1.3079	−0.502	1.0154	−14.800	1.2569	−0.717	1.0144
2.8	−30.123	1.4104	−0.501	1.0114	−15.250	1.3499	−0.393	1.0115	−16.977	1.2913	−0.572	1.0111
3.0	−35.140	1.4540	−0.469	1.0105	−17.295	1.3830	−0.368	1.0105	−18.775	1.3187	−0.534	1.0103
3.2	−39.341	1.4870	−0.461	1.0102	−19.035	1.4080	−0.362	1.0103	−20.206	1.3398	−0.524	1.0101
3.4	−42.628	1.5109	−0.459	1.0102	−20.465	1.4262	−0.361	1.0102	−21.315	1.3555	−0.521	1.0100

the energy (see Tables IX and X), resulting in energies that are lower than the full CI calculation for bond length greater than 1.8 Å. The results from restricted CCSD(T), QCISD(T), and BD(T) methods do not seem reliable beyond the onset of the UBD-RBD instability. It is possible that iterative inclusion of the triple excitations may partially overcome this problem.

Figure 5 shows the differences between the unrestricted CCSD, QCISD, BD, and full CI energies with and without the corrections for triple substitutions. In the region where the RHF or RBD wave functions are stable, the restricted data are used in the plot; beyond the instability the unrestricted data are used. For CCSD and BD without the triple substitution, the differences increase and reach the maximum at ~2.0 Å, which is near the onset of the UBD-RBD instability. Beyond the instability, the differences decrease and reach values of less than 1 mhartree. For QCISD, the results are similar except for a local minimum about one-tenth of an angstrom beyond the onset of the UHF-RHF instability. The maximum values of the differences are 6.7, 5.8, and 7.6 mhartree for CCSD, QCISD, and BD, respectively. For the calculations with triples, a small bump is found in the UCCSD(T) and UBD(T) curves at ~1.6 Å and a larger feature at ~2.2 Å for all three methods. These are associated with maxima in the triples corrections near 1.8–2.0 Å.

Replogle and Pople[25] compared QCISD and BD methods for the potential energy curve for the CH bond dissociation in methane with the STO-3G basis set. Depending on which solution was lower in energy, either a restricted or an unrestricted reference was used (i.e., the same as in Fig. 5). They found that QCISD(TQ) and BD(TQ) (where Q indicates noniterative corrections for quintuple excitations) are superior to QCISD(T) and BD(T), which in turn are better than QCISD and BD.

Spin projection has been shown to be very effective in the UMP4 calculations. In a previous paper[19] we proved that CCSD energies with and without single annihilation based on Eq. (16) are identical. The same theorem holds for QCISD and BD energies. Hence, single annihilation will not affect the CCSD, QCISD, and BD potential energy curves. Since unrestricted calculations on single bond dissociation energy curves have only one major spin contaminant, multiple spin annihilation is expected to have very little effect on

TABLE X. Triples contribution to the correlation energy ΔE_T (in mhartree) and normalization factor A_{norm} for $CH_4 \rightarrow CH_3+H$.

	RCCSD		UCCSD		RQCISD		UQCISD		RBD		UBD	
R(Å)	ΔE_T	A_{norm}	ΔE_T	A_{norm}	ΔE_T	A_{norm}	ΔE_T	A_{norm}	ΔE_T	A_{norm}	ΔE_T	A_{norm}
0.757	−3.335	1.0315			−3.245	1.0315			3.411	1.0312		
1.086	−3.630	1.0337			−3.508	1.0337			3.726	1.0334		
1.25	−3.877	1.0359			−3.617	1.0359			3.997	1.0355		
1.50	−4.522	1.0422			−4.239	1.0424			4.692	1.0413		
1.75	−5.701	1.0548	−5.646	1.0960	5.140	1.0551	−7.232	1.1061	5.897	1.0524		
2.00	−7.703	1.0773	−8.194	1.1498	6.542	1.0778	−7.721	1.1708	7.758	1.0713		
2.25	−10.890	1.1131	−7.197	1.1274	8.531	1.1132	−7.295	1.1383	10.332	1.0999	−10.328	1.0999
2.50	−15.578	1.1638	−4.962	1.0726	11.117	1.1616	−4.833	1.0745	13.531	1.1382	−6.002	1.0681
2.75	−21.794	1.2262	−3.397	1.0417	14.178	1.2185	−3.292	1.0417	17.101	1.1830	−3.603	1.0401
3.00	−28.953	1.2924	−2.861	1.0321	17.456	1.2763	−2.785	1.0321	20.689	1.2288	−2.946	1.0315
4.00	−51.156	1.4761	−2.654	1.0289	27.732	1.4281	−2.594	1.0289	31.100	1.3548	−2.708	1.0285

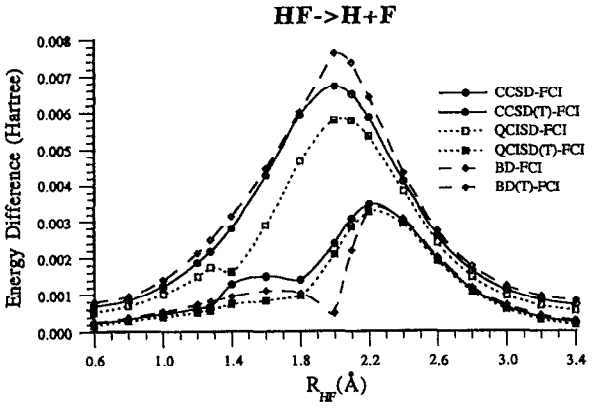

FIG. 5. Energy differences between various levels of theory and full CI for HF→H+F. Restricted methods used in the regions where the RHF and RBD wave functions are stable; unrestricted methods used otherwise.

the UCCSD, UQCISD, and UBD single bond dissociation curves.

Tables IX and X give the noniterative correlation correction from triple substitutions, ΔE_T, as well as the normalized factor $A_{\text{norm}} = \sqrt{1+\Sigma(a_i^a)^2+\Sigma(a_{ij}^{ab})^2}$ for the CCSD, QCISD, and BD calculations for HF→H+F and CH_4→CH_3+H, respectively. As mention above, ΔE_T for the restricted calculations increase with the bond length because large amplitudes are needed for single and double substitutions to remove the ionic contributions in the RHF reference determinant for H+F and CH_3+H. The maximum values of ΔE_T for the UBD calculations are at the onset of the UBD-RBD instability for both systems. The maxima of ΔE_T for UCCSD and UQCISD are at ~1.8 and 2.0 Å for HF→H+F and CH_4→CH_3+H, respectively. The correlation energies from the triple substitutions for these methods are three to ten times higher at the maxima than the values at either the well bonded structures or well separated structures.

The value of A_{norm} is a good indicator of the magnitude of the correlation correction for single reference determinant methods.[26] Tables IX and X show that A_{norm} increases with the bond length for restricted CCSD, QCISD, and BD. However, for unrestricted CCSD, QCISD, and BD, A_{norm} increases up to a bond length of 1.8–2.0 Å and then decreases at longer distances to values similar to those found near equilibrium geometries. For these systems UCCSD(T), UQCISD(T), and UBD(T) give better energies than the corresponding restricted method if A_{norm} for the restricted method is greater than 1.2. This may also be useful for judging the quality of the restricted vs unrestricted calculations for other systems.[26]

SUMMARY

The conclusions of this paper can be summarized in the following points:

(a) The value of S^2 is a useful diagnostic tool to determine the quality of post-SCF calculations. For H–F and CH_3–H bond dissociation curves, the onset of the UBD-RBD instability occurs near S^2=0.35 for the UCCSD or UQCISD calculations. The maxima in the errors for UMP4, UCCSD(T), UQCISD(T), and UBD(T) are at the region where S^2 is 0.5–0.6.

(b) For the cases considered, the differences in S^2 computed by $\langle\Psi_0|S^2|\Psi\rangle$ and $dE(\lambda S^2)/d\lambda$ are less than 0.005 for CCSD and QCISD calculations. The values of S^2 for QCISD computed with and without the T_1T_2 term differ by less than 0.005.

(c) Although they are based on UHF orbitals, the behavior of UCCSD and UQCISD is closer to BD than MP4, as judged by the potential energy curves and S^2.

(d) For dissociation of a single bond, the approximate spin projected MP4 energy [Eq. (19)] is in good agreement with the full CI energy. In the recoupling region (between the onsets of the UHF-RHF and UBD-RBD instabilities), the iterative methods such as CCSD(T), QCISD(T), and BD(T) give better results.

(e) The restricted and unrestricted calculations of CCSD(T), QCISD(T), and BD(T) give about the same errors compared with the full CI calculation between the onsets of the UHF-RHF and UBD-RBD instabilities.

(f) Although spin projection greatly improves the UMPn energies, it is not expected to have a large effect on CCSD, QCISD, and BD energy curves for the single bond dissociation.

(g) For single bond dissociation, single spin annihilation results are very close to full projection; however, for the system involving the breaking of two single bonds or a double bond, annihilation of at least two spin contaminants is necessary.

(h) For A_{norm}>1.2 in single bond dissociations, it is better to use a spin-unrestricted method.

ACKNOWLEDGMENT

This work was supported by a grant from the National Science Foundation (Grant No. CHE 90-20398).

[1] J. A. Pople and R. K. Nesbet, J. Chem. Phys. **22**, 571 (1954).
[2] C. Møller and M. S. Plesset, Phys. Rev. **46**, 618 (1934).
[3] For a review of many-body perturbation theory and coupled-cluster methods, see R. J. Bartlett, Annu. Rev. Phys. Chem. **32**, 359 (1981).
[4] J. A. Pople, M. Head-Gordon, and K. Raghavachari, J. Chem. Phys. **87**, 5968 (1987).
[5] N. C. Handy, J. A. Pople, M. Head-Gordon, K. Raghavachari, and G. W. Trucks, Chem. Phys. Lett. **164**, 185 (1989).
[6] See, for example, W. J. Hehre, L. Radom, P. Schleyer, and J. A. Pople, *Ab Initio Molecular Orbital Theory* (Wiley-Interscience, New York, 1986).
[7] C. C. Roothaan, Rev. Mod. Phys. **23**, 69 (1951).
[8] I. J. Carmichael, J. Phys. Chem. **95**, 108 (1991), and reference cited therein.
[9] D. M. Chipman, J. Chem. Phys. **94**, 6632 (1991), and references cited therein.
[10] M. J. Frisch, G. W. Trucks, M. Head-Gordon, P. M. W. Gill, J. B. Foresman, M. W. Wong, B. G. Johnson, H. B. Schlegel, M. A. Robb, E. S. Replogle, R. Gomperts, J. L. Andres, K. Raghavachari, J. S. Binkley, C. Gonzalez, R. L. Martin, D. J. Fox, D. J. Defrees, J. Baker, J. J. P. Stewart, and J. A. Pople, GAUSSIAN 92 (Gaussian Inc., Pittsburgh, PA, 1992).
[11] For a review of MCSCF methods, see Adv. Chem. Phys. **69**, 63 (1987).
[12] R. D. Amos, J. S. Andrews, N. C. Handy, and P. J. Knowles, Chem. Phys. Lett. **185**, 256 (1991).
[13] P. J. Knowles, J. S. Andrews, R. D. Amos, N. C. Handy, and J. A. Pople, Chem. Phys. Lett. **186**, 130 (1991).

[14] M. Rittby and R. J. Bartlett, J. Phys. Chem. **92**, 3033 (1988).
[15] P.-O. Löwdin, Phys. Rev. **97**, 1509 (1955).
[16] T. Amos and G. G. Hall, Proc. R. Soc. London Ser. A **263**, 483 (1961).
[17] H. B. Schlegel, J. Chem. Phys. **84**, 4530 (1986).
[18] P. J. Knowles and N. C. Handy, J. Phys. Chem. **92**, 3097 (1988).
[19] H. B. Schlegel, J. Phys. Chem. **92**, 3075 (1988).
[20] G. E. Scuseria and H. F. Schaefer III, J. Chem. Phys. **90**, 3700 (1989).
[21] D. M. Hirst, Chem. Phys. Lett. **122**, 225 (1985).
[22] J. A. Pople, M. Head-Gordon, and K. Raghavachari, J. Chem. Phys. **90**, 4635 (1989).
[23] G. D. Purvis, H. Sekino, and R. J. Bartlett, Collect. Czech. Chem. Commun. **53**, 2203 (1988).
[24] N. Koga, K. Yamashita, and K. Morokuma, Chem. Phys. Lett. **184**, 359 (1991).
[25] E. S. Replogle and J. A. Pople (in preparation).
[26] Lee and Taylor have a similar discussion, see T. J. Lee and P. R. Taylor, Int. J. Quantum Chem. Symp. **23**, 199 (1989).